

See discussions, stats, and author profiles for this publication at: <https://www.researchgate.net/publication/231639754>

Droplet Formation in a Ternary-Fluid Mixture: Spontaneous Emulsion and Micelle Formation†

ARTICLE *in* THE JOURNAL OF PHYSICAL CHEMISTRY A · JUNE 2004

Impact Factor: 2.69 · DOI: 10.1021/jp049112t

CITATIONS

7

READS

13

1 AUTHOR:



[Søren Toxvaerd](#)

Roskilde University

130 PUBLICATIONS **3,122** CITATIONS

SEE PROFILE

Droplet Formation in a Ternary-Fluid Mixture: Spontaneous Emulsion and Micelle Formation[†]

S. Toxvaerd*

Department of Chemistry, H. C. Ørsted Institute, DK-2100 Copenhagen Ø, Denmark

Received: February 27, 2004; In Final Form: May 17, 2004

A model of a ternary mixture, which in a qualitative way describes an organic solute in water in the presence of an amphiphilic component is simulated by molecular dynamics. The system is cooled, and the separation of droplets shows that the amphiphilic molecules can separate together with the organic solute in various ways. At onset of nucleation and for moderate strength of amphiphilicity the critical nucleus contains both species, but at later stage of this segregation the droplets are emulsionlike with subdomains in the droplets of only one of the two species. When the strength of affinity to the organic solute is increased, the amphiphile molecules are concentrated in the water droplet interface as in a micelle. We argue that D-glyceraldehyde, which is only moderately soluble in water and which has played a crucial role in evolution, together with organic materials is a candidate for such an emulsionlike droplet separation.

I. Introduction

Classical nucleation theory (CNT) has been very useful for the description and understanding of nucleation. In CNT the excess Gibbs free energy, ΔG^* , of formation of a nucleus is given by its bulk and surface terms,^{1,2} and CNT models for more complex systems beyond two-body force fields demonstrate the success of applying mean-field models and equilibrium thermodynamics to the nucleating process. Simulations of nucleation in simple systems of Lennard-Jones particles have confirmed CNT^{3,4} and provided information on a molecular level about the onset of nucleation as well as the dynamics of the phase separation. Many experiments of nucleation in gases are performed in the presence of inert particles and CNT assumes, and simulations demonstrate,⁵ that these inert particles do not participate in creation of the critical nucleus. On the other hand, droplet formation in liquid mixtures often take place in the presence of a third component, which is not inert but amphiphilic with respect to the two other immiscible components. This article contains molecular dynamics (MD) simulations of droplet formation in a ternary-fluid mixture. The mixture describes in a qualitative way a ternary mixture of water, where a solute of organic molecules separates by droplet formation in the presence of amphiphiles.

Nucleation in the presence of amphiphilic molecules has been the subject of intense experimental, theoretical, and numerical studies.⁶ The amphiphilic molecules are typically surfactantlike with hydrophilic heads and hydrophobic tails of, for example, lipids, and the simulations of phase separation in the presence of surfactants all show a late time behavior in accordance with experimental observation and with the surfactants concentrated in the interfaces,^{7–12} whereby the phase growth is slowed.⁸ In the case of droplet formations the resulting “micelles” will consist of a surfactant-rich surface.

The ideas of hydrophilicity, amphiphilicity, and hydrophobicity have been discussed for a long time.^{13–15} They play the crucial role in understanding of self-assembly of bio-organic matter. Whereas the hydrophilicity to water is well understood,

however, it is not the case with the interplay with lipids given by the hydrophobicity and the amphiphilicity. When it comes to amphiphilicity, it is always described as a surfactantlike quality, even when the amphiphilic property is given by simple spherical “Janus” molecules.¹⁶

The motivation for the present investigation is to investigate the droplet formation of organic materials in the presence of 2,3-dihydroxypropanal, or glyceraldehyde (GLA). GLA is indeed a compact Janus-like molecule with a part of its (surface) consisting of three hydrophilic functional groups. It is, however, only moderately soluble in water (3 g in 100 mL at 20 °C) despite its hydrophilic groups. Even one of the three groups should be enough to ensure solubility, as is the case for acetone, 1-propanol, and 2-propanol, which are totally miscible with water at room temperature, and propanal is 10 times more soluble in water than GLA. But the solubility is drastically reduced when all three functional groups are present together. Thus GLA is rather insoluble for another reason. The reason is its “self-philicity”. (This philicity is unique because its “dimer” α -D-glucose is about 30 times more soluble in water than GLA.) GLA is especially interesting since it is the simplest sugarlike molecule with an asymmetric carbon atom, and it is argued that it has played a central role in evolution.^{17,18} The hypothesis in refs 17 and 18 is that the excess pressure in droplets containing GLA results in a “domain-catalyzed” stereospecific ordering.

In the present article it is shown by MD that such a compact amphiphilic component also can separate together with the organic component in an emulsionlike manner. At onset of nucleation, both components are present in the interior of the nucleus, but as the droplet grows, the organic and the amphiphilic particles separate within the droplet in an emulsionlike manner with subdomains that contain only one of the components.

The model and the molecular dynamics (MD) details are given in section II, the results are given in section III, and section IV contains a short discussion.

II. Interaction Model and Simulation Technique

The system with droplet segregation is set up in order to simulate, in a qualitative way, the droplet formation of a bio-

[†] Part of the “Gert D. Billing Memorial Issue”.

* E-mail address: tox@st.ki.ku.dk.

TABLE 1: Values of the Cutoff Distances of the Pair Potentials in Eq 1^a

	W	O	GLA
W	2.5	$2^{1/6}$	$[2^{1/6}, 2.0]$
O	$2^{1/6}$	2.5	$[2^{1/6}, 2.0]$
GLA	$[2^{1/6}, 2.0]$	$[2^{1/6}, 2.0]$	2.5

^a Values are given in units of σ .

organic lipophilic solute (O) and a (compact) amphiphilic component (GLA) with affinity to O and to the solvent water (W) particles. The system is taken at a high temperature above the consolute temperature of a W/O mixture and quenched to a low temperature where O separates from W. In most of the simulations the amphiphilic GLA particles are taken to be moderately soluble in both phases but with various degrees of amphiphilicity. All these qualities can be ensured in a simple way by choosing different pair potentials between the species. In the simulations all three constituents interact via Lennard-Jones potentials (LJ), and the solubility are ensured only by varying the range of attractions between the particles by truncating the pair potentials. The LJ potential is usually truncated and set to zero for distances bigger than a cutoff distance, $r(\text{cut})$, which is traditionally set to $r(\text{cut}) = 2.5\sigma$ in most MD simulations of simple systems:

$$u_{ij}(r_{ij}) = u_{\text{LJ}}(r_{ij}) = 4e \left[\left(\frac{\sigma}{r_{ij}} \right)^{12} - \left(\frac{\sigma}{r_{ij}} \right)^6 \right] - u_{\text{LJ}}[r_{ij}(\text{cut})] \quad (1a)$$

if $r_{ij} < r_{ij}(\text{cut})$ and

$$u_{ij}(r_{ij}) = u_{\text{LJ}}(r_{ij}) = 0 \quad (1b)$$

if $r \geq r_{ij}(\text{cut})$.

The values of $r(\text{cut})$ used in the simulations are given in Table 1. The total loss of attractive forces between the solute W particles and the solvent O particles by taking $r_{\text{W,O}}(\text{cut}) = 2^{1/6}\sigma$ results in immiscibility below a consolute temperature $T_c \approx 4.7\epsilon/k$ for a three-dimensional system.¹⁹ The strength of amphiphilicity of GLA particles is given by the range of attraction to the W and O particles, which is determined for various values of $r(\text{cut})$ in the interval $[2^{1/6}\sigma, 2.0\sigma]$. The GLA particles have phobicity to the other constituents for $r(\text{cut}) = 2^{1/6}\sigma$, whereas they have complete philicity to the other species for $r(\text{cut}) = 2.5\sigma$.

A binary mixture of W and O particles will separate into two phases if it is cooled from a high temperature to a temperature below the consolute temperature. For an equal amount of solvent and solute particles, a so-called critical quench, the quench will lead to a spinodal decomposition with a given set of critical growth laws for the growth of the phases. For particle fractions with a dominating solvent, however, the separation will be different, and the growth of the new phases will be Lifshitz–Slyozov-like,²⁰ where the domain size of the droplets according to MD^{8,18,21} grows in mean proportional to time $t^{1/3}$ by droplet coalescence (Ostwalds ripening). It is this morphology, but for a ternary mixture including the amphiphilic GLA particles, which is investigated by choosing a particle fraction of the solvent $x_{\text{W}} = 0.9$. These quench of diluted solutions will also result in a separation of droplets. At late stage the droplets are found to grow in mean according to the Lifshitz–Slyozov law, and the systems end in a complete phase separation with one big droplet.

The system consists of $N_{\text{tot}} = 40\,000$ Lennard-Jones (LJ) particles in a cubic box with periodic boundaries. The solvent have $N_{\text{W}} = 36\,000$ LJ particles and the solute consist of $N_{\text{O}} =$

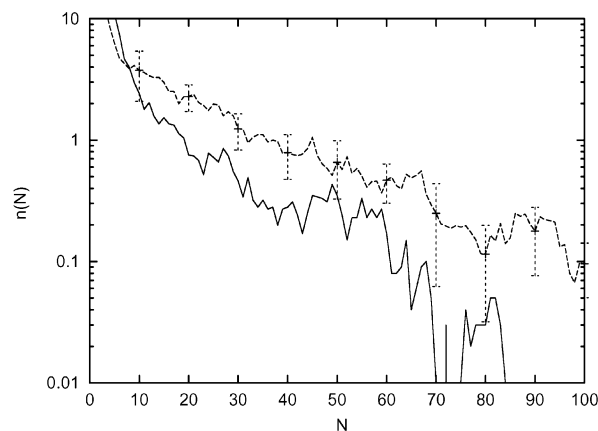


Figure 1. Mean number of clusters, $n(N)$, in the mixtures at onset of nucleation, as a function of numbers of particles, N , in the clusters [as $\ln n(N)$]. The solid line shows the distribution in a *binary* mixture with “organic” O particles only. The dashed line and error bars are the corresponding mean distribution in the ternary mixture of nucleating W and O particles, obtained from 10 simulations.

2000 and $N_{\text{GLA}} = 2000$ particles, respectively. The density is $\rho\sigma^3 = 0.80$, which corresponds to condensed liquid. The solutions are quenched from a high temperature $kT/\epsilon = 6$, above the consolute temperature of a W/O mixture to a temperature $kT/\epsilon = 1$ where the O particles separate in droplets. For MD computational details see ref 22. The droplets are identified as clusters of bounded O and GLA particles accordingly to Stillinger’s definition.^{4,23}

III. Droplet Formation in the Presence of Amphiphiles

A series of quenches with various range of attractions of the GLA particles to W and O particles, given by $r_{\text{GLA,W}}(\text{cut})$ and $r_{\text{GLA,O}}(\text{cut})$, show that $r(\text{cut}) \approx 1.5\sigma$ is a threshold value for the morphology of droplet separation. The attractive energy per particle in an uniform fluid state is given by the integral over the product of the radial distribution function, $g(r)$, and the pair potential as

$$u_{\text{attr}} = \frac{1}{2} \int_{2^{1/6}\sigma}^{\infty} dr \rho g(r) u(r) \quad (2)$$

and for a cutoff of the potential at 1.5σ it is reduced to about 40% of its value for $r(\text{cut}) = 2.5\sigma$. The GLA particles separate independently of the O particles by their own droplet condensation for smaller values of $r(\text{cut})$ than 1.5σ . On the other hand, the GLA molecules are soluble in the droplets if $r_{\text{GLA,O}}(\text{cut}) \geq 2.0\sigma$, and then one obtains a condensation with droplets of a rather homogeneous mixture of the two species. The attractive energy per particle in an uniform fluid state and with $r(\text{cut}) = 2.0\sigma$ is about 80% of its value for $r(\text{cut}) = 2.5\sigma$. The effect of the amphiphilicity of GLA on droplet separation shows up in the range $r_{\text{GLA,W}}(\text{cut}) \approx r_{\text{GLA,O}}(\text{cut}) \in [1.5\sigma, 2.0\sigma]$. In this range of amphiphilicity the droplet formation and phase separation appears as a corporative separation of O and GLA particles but with a nonuniform distribution of the two species at late times of separation. We shall first describe the onset of nucleation in the presence of the GLA amphiphiles.

Droplet formation appears as a nucleation from a metastable state for the present degree of supersaturation and with a critical nucleus of 50–100 particles, determined from the distribution of clusters in the supersaturated and metastable state.⁴ Figure 1 shows the mean distributions of clusters at the onset of nucleation and for $r_{\text{GLA,W}}(\text{cut}) = r_{\text{GLA,O}}(\text{cut}) = 1.5\sigma$ (dashed line), obtained from 10 simulations. Also shown is the distribution

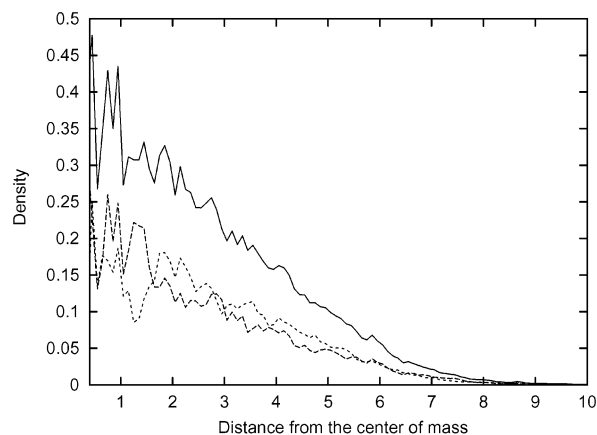


Figure 2. Density of O and GLA particles in the small droplets just after onset of nucleation as a function of the distance from the center of mass. (The GLA particles have a $r(\text{cut}) = 1.5\sigma$ to both O and W particles.) The density of the GLA particles is shown by long dashes and the density of the O particles by short dashes. The solid line shows the total density of the nucleating O and GLA particles.

of clusters in a *binary* mixture of only the O particles (solid line). A corresponding binary mixture of only amphiphilic W particles with $r_{\text{GLA,W}}(\text{cut}) = 1.5\sigma$, however, does not segregate. In a ternary mixture, however, both components segregate, but together although the size of the stable critical nucleus is increased, as indicated from the figure. The distribution of O and GLA particles in the critical nucleus is shown in Figure 2 and explains the result from Figure 1. If nucleation takes place from a metastable gas phase in the presence of inert particles, these particles do not contribute to the stability of the critical nucleus⁵ in accordance with classical nucleation theory.²⁴ But here the critical nucleus contain a core with a relatively high particle fraction (≈ 0.5) of the amphiphiles. This property is demonstrated in Figure 2, which shows a representative example of the density profiles of the two species in the nucleus just after the onset of nucleation. Within the accuracy of the simulations, the two species exhibit the same monotonic declining density profile just after the onset of nucleation with a ratio $\rho_{\text{GLA}}(r)/\rho_{\text{O}}(r) \approx 1$ and equal to the overall ratio of the two species in the ternary mixture. The two figures show that the O particles catalyze the phase segregation of amphiphiles, by that the amphiphiles separate together with the solute O particles in droplets, which grow in accordance with the Lifshitz–Slyozov law²⁰ for phase separation with droplet coalescence.

As the droplets grow, the density distribution for the GLA particles changes, however, from a monotonic declining function of the distance from the center of mass into a distribution with the amphiphiles located in the droplet interface and for a certain strength of affinity to the O particles, with a emulsionlike separation with subdomains of, respectively, GLA and O particles. The emulsionlike phase growth with separated subdomains of each species within a droplet appears for a certain strength of philicity, given by $r_{\text{GLA,O}}(\text{cut})$. For $r_{\text{GLA,O}}(\text{cut}) \in [1.5\sigma, 1.7\sigma]$, the mutual equilibrium solubility of GLA and O particles is small and a droplet contains a subvolume of a GLA phase and an O phase. [The attractive energy per particle in a uniform fluid state and with $r(\text{cut}) = 1.7\sigma$ is about 60% of its value for $r(\text{cut}) = 2.5\sigma$.] This fact does not, however, affect the Ostwalds ripening with growth via droplet collisions, as can be seen in the next figure. Figure 3 shows a fusion of two droplets at late time of the separation and for $r_{\text{GLA,O}}(\text{cut}) = 1.6\sigma$. Both droplets contain subdomains of each nucleating species before the collision. The positions of the GLA particles are

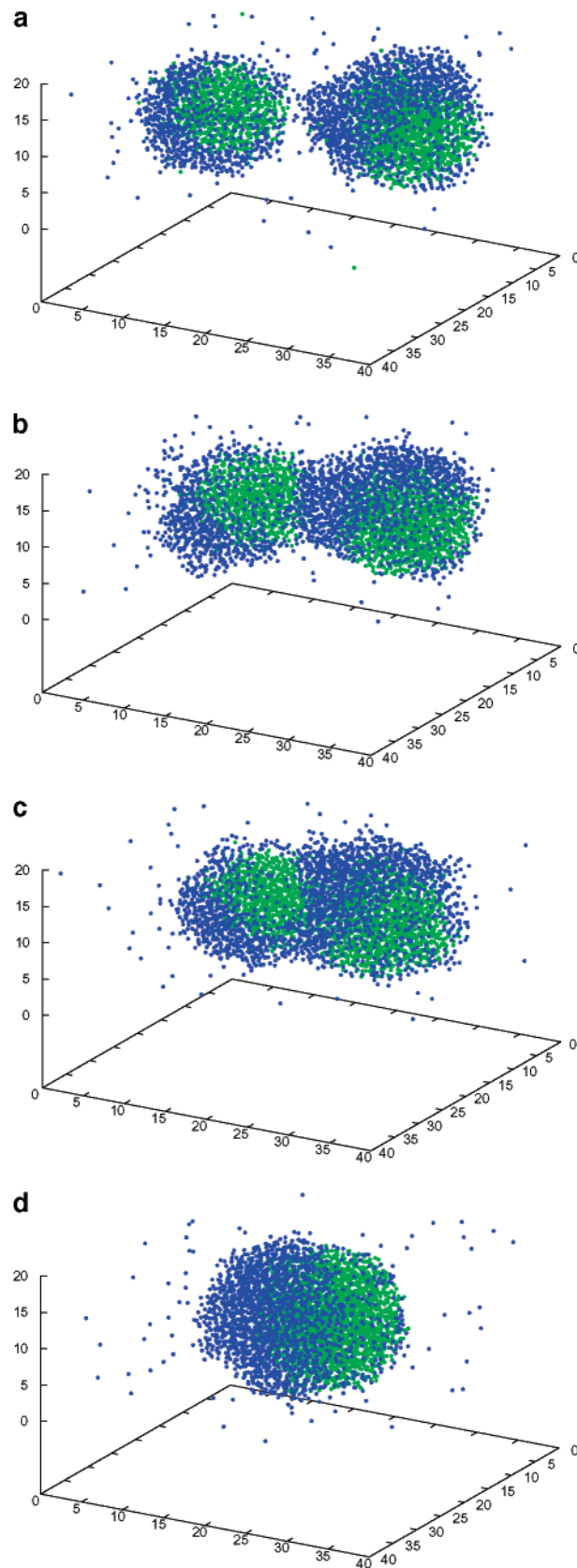


Figure 3. Collision of two droplets. The positions of GLA particles are shown by blue dots, and O particles, by green dots. (The solvent of W particles is not shown.) The droplet collision and fusion take place during $\approx 2 \times 10^4$ time steps (≈ 0.2 ns). Panels a–c show the particle positions with a time interval of 10^4 time steps. Panel d shows the positions in the droplet 10 ns after the fusion.

shown by blue dots, and the positions of the O particles with

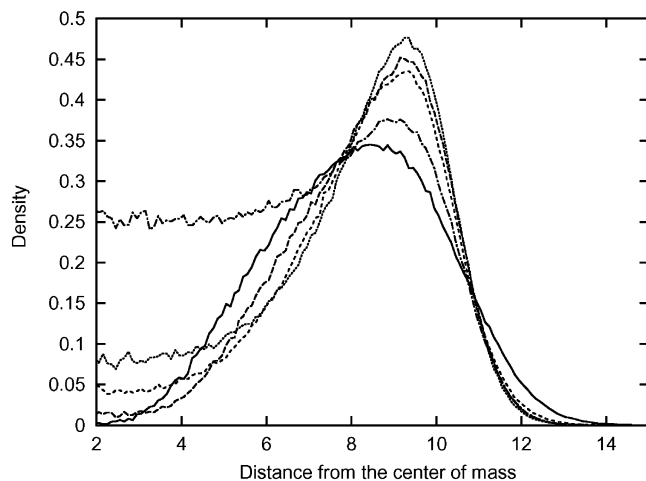


Figure 4. Density of GLA particles in the droplets at equilibrium as a function of the distance from the center of mass. The five profiles are for increasing affinities of amphiphile GLA particles to the O particles, given by the value of $r(\text{cut})$. The five curves are for $r(\text{cut}) = 1.5\sigma$, 1.6σ , 1.7σ , 1.8σ , and 2.0σ , respectively, and with increasing density of GLA particles in the center of the nucleus as the r_{cut} value is increased.

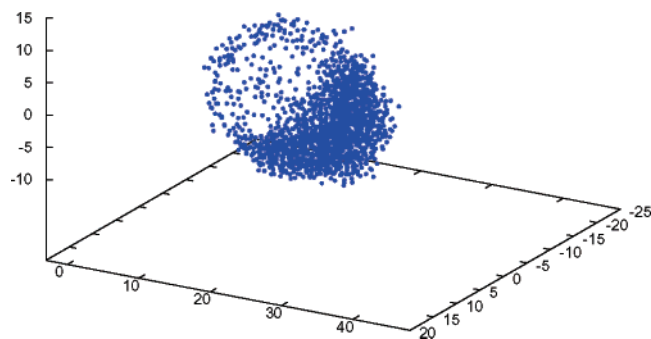


Figure 5. Distribution of GLA particles at equilibrium and for $r(\text{cut}) = 1.5\sigma$. The GLA particles perform their own subphase in the droplet and with some GLA particles in the remaining solvent–droplet interface.

green dots. Figure 3a–c shows the positions with time intervals of 0.2 ns, and Figure 3d is 10 ns after the fusion where the emulsionlike equilibrium distribution is reestablished.

The equilibrium distributions, given by $\rho_{\text{GLA}}(r)$, of GLA particles in a droplet of ≈ 2000 GLA particles and 2000 O particles are shown in Figure 4. The equilibrium were reached after ≈ 50 ns. The five functions are for $r_{\text{GLA,O}}(\text{cut}) = 1.5\sigma$, 1.6σ , 1.7σ , 1.8σ , and 2.0σ and with an increasing density in the center of the droplet as the $r(\text{cut})$ value is increased. The shoulder in $\rho(r)$ for $r_{\text{GLA,O}}(\text{cut}) = 1.5\sigma$ is due to the separation into the two subdomains, but when the amphiphilicity is increased the GLA particles are also spread in the interface between the droplet and the water phase of W particles in a micellelike structure.

Figure 5 shows a set of positions of the GLA particles in the droplet at equilibrium and for $r_{\text{GLA,O}}(\text{cut}) = 1.5\sigma$. The GLA particles are mainly located in a subdomain of the droplet in an emulsionlike configuration for this strength of amphiphilicity to O but with a few of the GLA particles spread out in the water–droplet interface. The distributions of the GLA particles are, however, more micellelike for increasing strength of affinity to the O particles. For $r(\text{cut}) = 1.6\sigma$ and 1.7σ , the droplets still contain (bulk)subdomains of only GLA particles but with a coherent layer of GLA particles in the W/O interface. But although the distributions of the amphiphiles for these strengths

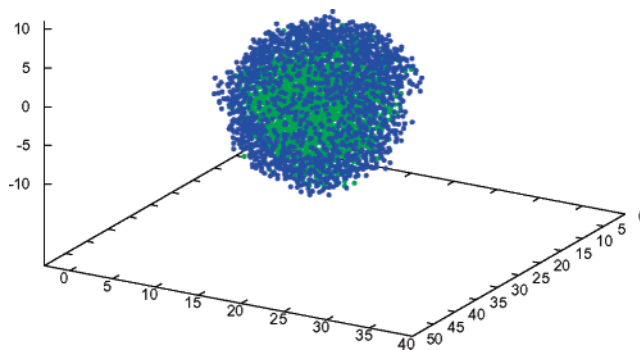


Figure 6. Distribution of GLA particles (blue) and O particles (green) at equilibrium and for $r(\text{cut}) = 1.7\sigma$. The GLA particles still perform their own subphase in the droplet and almost wet the W/O interface.

of affinity to O remain about prewetting^{25,26} of the subdomain of the O-rich part of the droplet, this part is not totally covered by GLA particles as shown in Figure 6, and the distributions, shown in Figures 4–6 just demonstrate that the amphiphiles have a affinity to themselves but that they also are soluble in the solvent–droplet interface. The GLA particles are solvable in the O phase for $r(\text{cut}) \geq 2.0\sigma$ but with an enhanced concentration in the solvent–droplet interface (Figure 4).

IV. Discussion

The simple and qualitative model for droplet separation of lipophilic O components in the presence of GLA-like amphiphiles shows that the droplet formation exhibits complex behavior. The droplet segregation covers independent phase separations of, respectively, O and GLA particles for weak amphiphilicity and a corporative and emulsionlike separation for moderate amphiphilicity, with both species present in the core of the critical nucleus at the onset of nucleation. But during the segregation the two components separate in subdomains. For strong philicity to the organic phase, the amphiphiles and the organic compound are miscible, but still with an enhanced concentration of the amphiphiles in the solvent–droplet interface.

Glyceraldehyde (GLA) is amphiphilic in the sense that it is moderately soluble in water and in an organic solvent. The present investigation shows in a qualitative way that such amphiphiles might separate together with hydrophobic compounds in water, in various ways including emulsionlike separation and micelle formation. A commonly used bio-organic solvent is 1-octanol. The distribution coefficient for GLA in a water/1-octanol system at 25 °C has been measured for different concentrations of GLA (1, 2, 4, and 8 mg/mL) and is ≈ 1 (mole fraction).²⁷ A distribution coefficient equal to 1 is obtained in the present qualitative model for the ternary mixture when the GLA has the same attractive energy per GLA particle in a (diluted) solution of the two solvent (W and O). This is ensured by having the same $r(\text{cut})$ in the pair potentials to W and O, respectively. For a reduced attractive energy to W and O of 40% to 75% (corresponding to $r(\text{cut}) \in [1.5, \approx 1.7]$) we observe an emulsionlike droplet formation but with the amphiphilic GLA also spread in the droplet interface in a surfactantlike manner (Figures 3, 5, and 6).

The possibility of an emulsionlike separation with subdomains containing only the amphiphiles is crucial for the stereospecific ordering described in refs 17 and 18. If a multicomponent mixture of organic components including GLA is cooled and performs this kind of phase segregation, the GLA can undergo an ordering into one of its enantiomer configurations, by a domain-catalyzed isomerization kinetics of the molecules in the

GLA subdomain, At the same time the GLA molecules are present in a coherent layer in the interface between the hydrophobic components and water, where they can act as the seeds for synthesis of glycerides and phosphoglycerides. Once they react, for example, with carboxylic acids by creation of esters (at carbon atom 2), the resulting molecules behave as stereospecific surfactants (the keto–enol isomerization kinetics is then turned off) and will maintain in the interface and stabilize and ensure the micelle structure. Only real experiments (or a much more realistic force field for three components in ternary mixture and with isomerization kinetics included) can test this hypothesis. Many thermodynamical and biochemical facts, however, do support the ideas that the homochirality of not only sugar but also L-amino acids is originated from D-GLA.^{28,29} In ref 28 it is found that D-GLA only couples with L-sarime in a racemic mixture, and in ref 29 it is correspondingly found that L-sarime couples stereospecifically with other L-amino acids. The results link the L-amino acids with D-sugar via GLA. GLA is the central anchor molecule in the glycerides and phosphoglycerides, which are the “brick” molecule in membranes and a central molecule in the glycolysis, so it must necessarily have played a central role in evolution.

There is of course a very, very long route of self-assembly from simple emulsionlike droplets with a stereospecific ordering of their surfaces of GLA and glycerides to even the simplest prokaryote with double-layered membrane, with a very complex cytokinesis (cell division) and with a metabolism. The present article and refs 17 and 18 offer a possible explanation of the very first steps on this route.

Acknowledgment. I am grateful to Peter Westh for measurements of the solubility of GLA. My late colleague Gert Due Billing is gratefully acknowledged.

References and Notes

- (1) Reiss, H. *J. Chem. Phys.* **1950**, *18*, 840.
- (2) Katz, J. L. *J. Chem. Phys.* **1970**, *52*, 4733.
- (3) ten Wolde, P. R.; Frenkel, D. *J. Chem. Phys.* **1998**, *109*, 9901.
- (4) Toxvaerd, S. *J. Chem. Phys.* **2001**, *115*, 8913.
- (5) Toxvaerd, S. *J. Chem. Phys.* **2003**, *119*, 10764.
- (6) Kusaka, I.; Oxtoby, D. W. *J. Chem. Phys.* **2001**, *115*, 4883 and references therein.
- (7) Smit B.; Hilbers, P. A. J.; Esselink, K.; Rupert, L. A. M.; van Os, N. M.; Schliper, A. G. *Nature* **1990**, *348*, 624.
- (8) Laradji M.; Mouritsen, O. G.; Toxvaerd, S.; Zuckermann, M. *Phys. Rev. E* **1994**, *50*, 1243.
- (9) Schmidt M.; von Ferber, C. *Phys. Rev. E* **2001**, *64*, 051115-1.
- (10) Lissal, M.; Hall C. K.; Gubbins, K. E. *J. Chem. Phys.* **2002**, *116*, 1171.
- (11) Imai, M.; Teramoto, T.; Teramoto, I.; Takahashi, I.; Nishiura, Y. *J. Chem. Phys.* **2003**, *119*, 3891.
- (12) Guo, H.; Kremer, K. *J. Chem. Phys.* **2003**, *119*, 9308.
- (13) Hildebrand, J. H. *Proc. Natl. Acad. Sci. U.S.A.* **1979**, *76*, 194.
- (14) Tanford, C. *Proc. Natl. Acad. Sci. U.S.A.* **1979**, *76*, 4175.
- (15) Hvidt, A.; Westh, P. *J. Sol. Chem.* **1998**, *27*, 395.
- (16) Erdmann, T.; Kröger, M.; Hess, S. *Phys. Rev. E* **2003**, *67*, 041209-1.
- (17) Toxvaerd, S. *Phys. Rev. Lett.* **2000**, *85*, 4747.
- (18) Toxvaerd, S. *J. Chem. Phys.* **2004**, *120*, 6094.
- (19) Toxvaerd, S.; Velasco, E. *Mol. Phys.* **1995**, *86*, 845.
- (20) Lifshitz, I. L.; Slyozov, V. V. *J. Phys. Chem. Solids* **1961**, *19*, 35.
- (21) Velasco E.; Toxvaerd, S. *J. Phys. Condens. Matter* **1994**, *6*, A205.
- (22) For MD details see Toxvaerd, S. *Mol. Phys.* **1991**, *72*, 159.
- (23) Stillinger, F. H. *J. Chem. Phys.* **1963**, *38*, 1486.
- (24) Fisk, J. A.; Katz, J. L. *J. Chem. Phys.* **1996**, *104*, 8649.
- (25) Fan, Y.; Monson, P. A. *J. Chem. Phys.* **1993**, *99*, 6897.
- (26) Toxvaerd, S. *J. Chem. Phys.* **2003**, *117*, 10303.
- (27) Westh, P. Unpublished results.
- (28) Takats, Z.; Nanita, S. C.; Cooks, R. G. *Angew. Chem.* **2003**, *42*, 3521.
- (29) Koch, K. J.; Gozzo, F. C.; Nanita S. C.; Takats, Z.; Eberlin, M. N.; Cooks, R. G. *Angew. Chem.* **2002**, *114*, 1797.